

A study of phenoxyl radicals of curcumin and related molecules by electron spin resonance spectroscopy

Colin T. Mason '28 and Herbert J. Sipe, Jr.

Department of Chemistry, Hampden-Sydney College, Hampden-Sydney, VA 23943

Abstract

Electron Spin Resonance spectroscopy revealed the presence of phenoxyl radicals from curcumin and substructures, including 4-tert-butylphenol (1), 4-vinylphenol (2), 4-hydroxybenzalacetone (3), ferulic Acid (4), bisdemethoxycurcumin (5), and curcumin (6). Curcumin and these related molecules all share the presence of phenolic hydroxyl structure, suggesting antioxidant properties. Given that free radicals are known to induce oxidative damage to essential cellular components, an ESR study was conducted on curcumin and related molecules to analyze their ability to generate phenoxyl radicals. The Electron Spin Resonance fast-flow technique was used to facilitate the studied compounds. Solutions of the studied compounds were prepared either at a concentration of 2.0 mM or 5.0 mM, while the oxidizing solution—cerium (IV) sulfate was dissolved in 0.225 M sulfuric acid—was prepared either at a concentration of 1.8 mM or 4.8 mM. These solutions flowed separately until meeting in the flat cell of the ESR, producing free radicals. Spectra were successfully recorded from all studied compounds using the ESR instrument. Experimental spectra were analyzed using the program known as WinSim, which provides the ability to extract hyperfine coupling constants. Density functional theory calculations were performed on all studied compounds, yielding theoretical hyperfine coupling constants. Using WinSim, hyperfine coupling constants were extracted for 4-tert-butylphenol, 4-vinylphenol, 4-hydroxybenzalacetone, ferulic Acid, and bisdemethoxycurcumin. Experimental HFCC were used to produce simulated spectra that closely matched the experimental spectra as indicated by correlation values “R” approaching 1.0. ESR spectra were obtained of curcumin derived radicals; however, the overall resolution of curcumin spectra were low, not permitting the ability to simulate them in WinSim.

Background Information

Free radicals are reactive molecules that contain an unpaired electron in their singly occupied molecular orbital. These species are paramagnetic and can be generated from either the gaining or losing a valence electron, increasing the molecules' reactivity.¹ Among the most biologically relevant free radicals are those classified as Reactive Oxygen and Nitrogen Species (RONS). Examples of RONS include nitric oxide ($\bullet\text{NO}$), alkoxy ($\bullet\text{OR}$), peroxy radicals ($\text{ROO}\bullet$), hydroxyl radicals ($\bullet\text{OH}$), hydrogen peroxide (H_2O_2), and superoxide ($\text{O}_2\bullet^-$). Specifically, superoxide ($\text{O}_2\bullet^-$) is a free radical and is a precursor molecule to radicals.² Moreover, natural phenolic compounds are found in many plants as secondary metabolites. Numerous natural phenolic compounds are in the human diet, either through normal consumption or intake of dietary supplements. These phenolic compounds are commonly considered antioxidants, as in low concentration they contain the ability to reduce the risk of various chronic and degenerative diseases including cardiovascular diseases, neurological diseases, and many types of cancers.³ However, under certain conditions, phenolic compounds can transition to prooxidants, inducing oxidative stress to vital cellular components. Prooxidant formation is especially pronounced in the presence of transition metal ions such as Cu^{2+} or Fe^{3+} . Through redox interactions, phenolic compounds reduce these metal ions while being oxidized to phenoxyl radicals. Furthermore, in oxygen rich

environments, phenoxyl radicals readily react with oxygen to produce superoxide anions ($\text{O}_2\bullet^-$). These superoxide species can further react with phenolic compounds to yield hydrogen peroxide (H_2O_2), which, in turn, participates in Fenton-like reactions with reduced metals to produce highly reactive hydroxyl radicals ($\bullet\text{OH}$).³ As a result, phenolic compounds in the presence of transition metals can produce various types of oxidative species that are known to cause lipid peroxidation, DNA fragmentation, cell death, DNA damage, changes in protein structure, and membrane damage.¹⁻³

Curcumin is a naturally occurring antioxidant and polyphenolic compound found in the rhizome of *Curcuma longa* (turmeric). Curcumin is known for its anti-inflammatory, antioxidant, anti-tumor properties, making it a subject of growing interest in both biomedical research and public health.⁴ Traditionally in Asia, curcumin has been used as a medical herb due to its antioxidant properties.⁵ Currently, curcumin is widely used as a culinary spice, a key ingredient in herbal dietary supplements, and a natural dye in textiles and food products. Clinical and preclinical studies suggest that curcumin contains therapeutic benefits for a range of inflammatory conditions, including inflammatory bowel disease, arthritis, psoriasis, depression, Alzheimer's disease, atherosclerosis and COVID-19.⁴⁻⁵

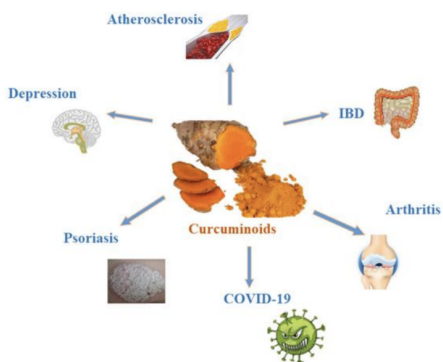


Figure 1: The claimed health benefits of curcuminoids, the family of curcumin molecules.⁴

Although curcumin has been demonstrated to have therapeutic benefits to various inflammatory conditions, the phenolic structure of the molecule and related molecules examined.⁶ In this study suggest a potential for phenoxyl radical formation. To observe this phenomenon, electron spin resonance spectroscopy was used to analyze curcumin and substructures.

Materials and Methods

Electron Spin Resonance (ESR) spectroscopy is a technique used for detecting paramagnetic species, operating by exposing unpaired electrons to microwave radiation within a strong external magnetic field.⁵ Electrons contain intrinsic angular momentum, known as spin, which is represented by the quantum number m_s . This spin can exist in one of two states: spin-up ($m_s = +1/2$) or spin-down ($m_s = -1/2$).⁶ In the absence of a magnetic field, the two possible spin states of an unpaired electron are equivalent in energy. This condition is known as degeneracy.⁵ However, when a magnetic field is applied, the degeneracy is lifted due to the Zeeman effect.⁶ The magnetic field interacts with the magnetic moment of the electron, causing the spin states to split into different energy levels. This results in non-degenerate spin states of unpaired electrons and resonance. When the energy difference between the two spin states equals the energy from the fixed microwave frequency, absorption occurs leading to an ESR signal.⁶ In addition, unpaired electrons have further interactions with nearby atomic nuclei if those nuclei have nonzero nuclear spins. These interactions are known as hyperfine coupling, and they provide further splittings of the ESR signal. Hyperfine coupling constants for nuclei with $I = 1/2$, ^1H hydrogen nuclei, follow the $n+1$ rule, as shown below in Figure 2.

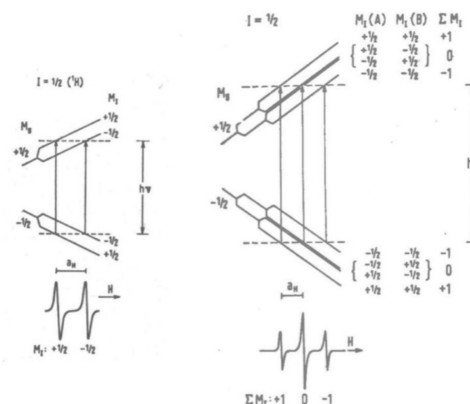


Figure 2: Shown above are hyperfine interactions involving one (left) and two equivalent hydrogen nuclei (right). The central energy difference between spin states ($h\nu$) represents the Zeeman splitting, caused by the external magnetic field. The additional splittings above and below this energy gap illustrate hyperfine coupling, following the $n+1$ rule: one nucleus yields a doublet, two equivalent nuclei yield a triplet.

A JEOL X-310 spectrometer was used to facilitate all experiments. The ESR spectrometer is composed of three main systems: the magnet subsystem, the microwave subsystem, and the modulation and detection subsystem.¹ First, the magnetic subsystem generates a magnetic field to align the electrons in a parallel orientation. Next, in the microwave subsystem, the Gunn Diode produces fixed microwave signals from its power supply. These microwaves travel through the microwave bridge and reference arm into the cavity, which is where the sample is located. To reduce potential noise in spectra, the automatic frequency control, or AFC, locks the microwave frequency to the resonant frequency of the cavity. Finally,⁷ the modulation and detection subsystem contain a 100KHz oscillator and amplifier, providing the sample with a small ripple field through cavity modulation coils. Additionally, a 100KHz phase detector selectively amplifies signal coded at 100KHz and suppresses signals at other frequencies.¹ Lastly, a phase shifter corrects phase lags between modulation of ESR signal and detection. A labeled ESR instrument block diagram is shown in Figure 3.

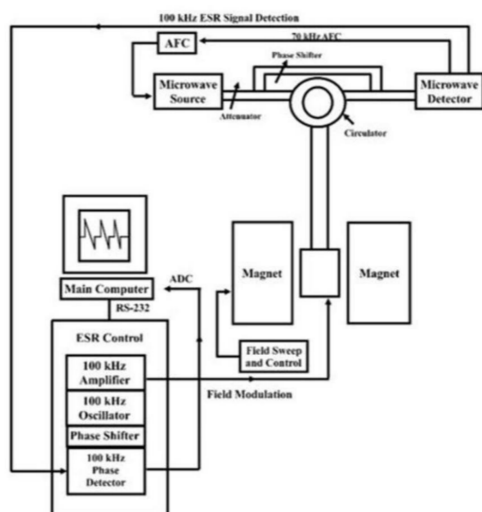


Figure 3: Block diagram of the ESR spectrometer, showing all the labeled components of the Instrument

ESR measurements were conducted using a fast-flow system. This methodology involves using low molarity solutions and mixing them, which generates free radicals within the specialized flat cell. The flat cell used in these experiments was specifically designed to enable the mixing of two separate solutions, allowing chemical reactions to occur during ESR Spectroscopy. A peristaltic pump was used to control the flow rate of the solutions into the flat cell. The ESR instrument records the ESR spectra that are produced. Then, the experimental ESR spectra can be analyzed in a software program called WinSim, where simulation spectra and optimizations can be made.¹⁰ Moreover, a correlation value is produced from the simulated spectra, recognized as R^2 ; a R^2 value of 1.0 is a perfect simulation in comparison to the experimental spectrum. A good and acceptable correlation is any value above 0.9. A residual spectrum can also be obtained in WinSim by subtracting the simulated spectrum from the experimental spectrum. This residual spectrum grants the ability to see what parts of the experimental spectrums were not a good fit for the simulation.

Density Functional Theory Calculations

Molecular orbital theory is interested in modeling the structure of molecules, especially their electrons.⁷ Density Function Theory (DFT) is a computational quantum mechanical modeling method used to investigate the electronic structure of a given molecule.⁸ While other methods such as Hartree-Fock would yield similar approximations, DFT was chosen because of software availability and the relatively low computational load.

Chemicals Studied

Curcumin, a structurally complex polyphenolic compound, complicates the interpretation of hyperfine coupling constants due to its numerous hydrogen nuclei, which can produce extensive splitting's in experimental ESR spectra. Therefore, investigating simpler substructures first enables a systematic approach to identifying HFCCs. This facilitates position-specific analysis across related molecules. Ultimately, identifying similarities in HFCC values at distinct chemical positions across related molecules enables more accurate analysis and assignment of HFCCs in Curcumin.

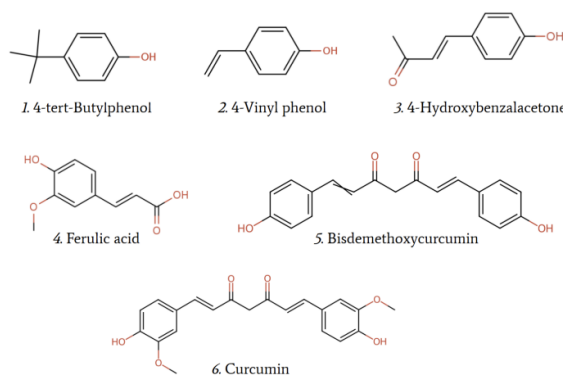


Figure 4: Above are the chemical structures of 4-tert-Butylphenol (1), 4-Vinyl phenol (2), 4-Hydroxybenzalacetone (3), Ferulic acid (4), Bisdemethoxycurcumin (5), Curcumin (6).

Chemicals and Solutions

Curcumin was purchased from Sigma Aldrich (St. Louis, MO). The bisdemethoxycurcumin was purchased from Tokyo Chemical Industry (Tokyo, Japan) Ferulic acid was purchased from AK Scientific. 4-Hydroxybenzalacetone was purchased from AK Scientific. 4-Vinyl phenol was purchased from AK Scientific. 4-tert-Butylphenol was purchased from AK Scientific. Cerium (IV) sulfate was purchased from Sigma Aldrich. 95% ethanol was purchased from Greenfield (Grayslake, IL). Finally, the sulfuric acid was purchased from Sigma Aldrich. For each experiment, two solutions were prepared. Depending on the compound, the solution containing the studied molecule had either a concentration of 2mM or 5mM, in 2 liters of DI water and 2 liters of 95% ethanol. For the 4-tert-butyl phenol, 4-vinyl phenol, bisdemethoxycurcumin, and curcumin experiments, a concentration of 2mM was used due to solubility or chemical amount concerns. For the 4-hydroxybenzalacetone and ferulic acid experiments with a concentration of 5mM were used for the studied molecule solutions. It is also important to note that 4-vinyl phenol was in a propylene glycol solution, so it had to be measured using a micro-pipet instead of an analytical balance like the other molecules. For the second solution, either a 1.8mM or 4.8mM cerium (IV)

sulfate concentration was used. For the 4-tert-butyl phenol, 4-vinyl phenol, bisdemethoxycurcumin, and curcumin experiments, a A concentration of 1.8mM cerium (IV) sulfate was used. For the 4-hydroxybenzalacetone and ferulic acid experiments, a concentration of 4.8mM cerium (IV) sulfate was used to match the concentration of the 5mM compound solutions. Along with the 1.8mM or 4.8mM cerium (IV) sulfate, 100ml of concentrated sulfuric acid, and 3,900ml of DI water were added, making the 30 cerium (IV) solutions 0.225M in sulfuric acid. Each solution required stirring via a magnetic stir bar on a stir plate.

ESR Experiments

The listed solutions above were placed into their own separate reservoir. The solutions were then bubbled with N₂ gas for five minutes. This was done to remove any paramagnetic oxygen dissolved in the solution. After five minutes of N₂ bubbling, the reservoirs were transferred to a tilting rack designed by Dr. Sipe and previous students. The tilting rack is adjacent to the ESR instrument and can be used to tilt the reservoirs as the volume decreases throughout the experiment to ensure proper solution flow. Rubber tubing was connected between the reservoirs and the flat mixing cell within the ESR instrument. A three-way valve is used to control the start and stop of solution flow from the fast flow reservoirs and control the flow of a third reservoir containing DI water. The DI water reservoir is used for initial tuning of the ESR instrument and cleaning of the tubing. Furthermore, a variable speed peristaltic pump serves as an intermediate between the fast flow reservoirs and the flat cell. The peristaltic pump controls the flow rate and sends the solutions to be mixed in the flat cell. After mixing in the flat cell, the diluted solution containing both fast flow reservoirs solutions would flow through a waste tube into a waste disposal container. Below, Figure 15 shows a diagram of the fast flow system, which was created by Brant Boucher in his summer research project from 2014.

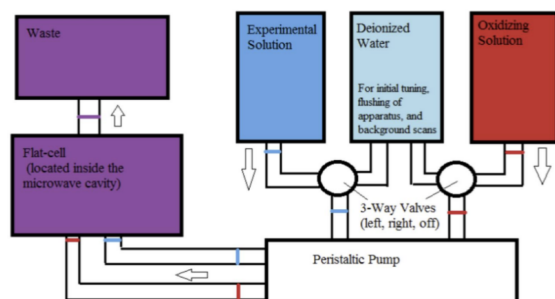


Figure 15: Boucher's diagram of the fast flow system.

The JEOL X-310 spectrometer was used for observing phenoxy radicals generated during the fast flow technique. With each experiment, the settings and parameters were adjusted to produce the best possible ESR signal, but the microwave cavity was modulated at a constant rate of 100 KHz. A software program was provided by JEOL, which operated the spectrometer and recorded experimental spectra. Additionally, WinSim, 2002, a software program designed by researchers from the NEIHS (Research Triangle Park, NC), was used to simulate the experimental spectra and extract hyperfine coupling constants. The JEOL software outputs recorded spectra in a format incompatible with the .lmb files required by WinSim for simulation. Consequently, a multi-step conversion process was implemented to transform the experimental spectra into a compatible format, enabling the ability to simulate spectra. First, the file was transformed into text data and shortened to 8K. Next, the text data was pasted into a text editor 32 where the file edited to remove excess data that was not necessary for WinSim, along with appropriately titling the file. Once editing was finished in the text editor the file was saved as a data file. From there, a locally written file converter program was used to change the data file to an .lmb file. Moreover, molecules had to be constructed strategically before submitting inputs for DFT calculations. So, a program called Gauss View '03 was used to build and articulate the molecules into phenoxy radicals before submitting them for DFT calculations. Gaussian '03, a program that works coherently with Gauss View '03, facilitated all DFT calculations.¹¹ Gaussian '03 was purchased from Cyberchem (Gainesville, Florida)

Discussion

4-tert-Butylphenol

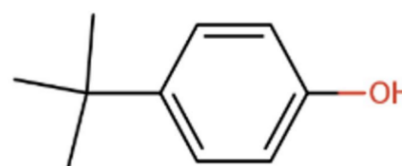


Figure 5: Chemical structure of 4-tert-Butylphenol.

Fast flow experimentation of 4-tert-butylphenol produced a signal in ESR indicating the

formation of radicals. The fast flow experiment consisted of two solutions. The first solution consisted of 2mM 4-tert-butylphenol in a 50/50 (v/v) ration solution of DI H₂O and 95% ethanol. The second solution consisted of 1.8mM Ce(SO₄)₂ in 0.225M concentrated H₂SO₄. Equivalent volumes were mixed in the flat cell, creating final concentrations of 1.0mM 4-tert-butylphenol and 0.9mM Ce(SO₄)₂. An ESR signal was observed at flow rates of 40mL/min, 60mL/min, 80mL/min, and 100 mL/min. A flow rate of 100 mL produced the best ESR signal, which can be seen in Figure 6(a). Additionally, Figure 6(b) shows the simulated spectrum in WinSim that has a correlation value of $R^2=0.956231$. Three distinct coupling constants were able to be extracted: $a^{\text{H}_i} = 6.08$ (2H), $a^{\text{H}_i} = 1.85$ (2H), $a^{\text{H}_{\text{CH}}} = 0.46$ (9H). Also, a second unresolved polymeric species was added to the simulation, since polymerization was possible. The parameters for species 1 are as follows: 66.313% relative concentration, 99.901G Lorentzian line shape, 0.326G line width, and 0.000G G-shift. The parameters for species 2 are as follows: 33.687% relative concentration, 123.145 Lorentzian line shape, 1.906G line width, and 0.000G G-shift. These parameters were optimized in WinSim software. In Figure 6(c) a residual spectrum is shown, which is generated 11 by subtracting the experimental spectrum from the simulated spectrum. The residual spectrum displays a moderate level of noise, which could be caused by the second species.

DFT calculations were facilitated using the “epr-ii” basis set, which is a variation of the 3-21G basis set. The calculations produced the following coupling constants: $a^{\text{H}_i} = 6.96$ (2H), $a^{\text{H}_i} = 2.59$ (2H), $a^{\text{H}_{\text{CH}}} = 0.81$ (9H).

These results are summarized in Table 1. These results demonstrate that through the chemical oxidation of 4-tert-butylphenol, stable phenoxyl radicals form that live long enough to be observed using specific parameters in our experimentation. All three experimental coupling constants are smaller than the values obtained through DFT calculations, demonstrating a theme. While the experimental coupling constants vary slightly from the coupling constants obtained by DFT calculations, they are close enough to validate our assignment of experimental coupling constants.

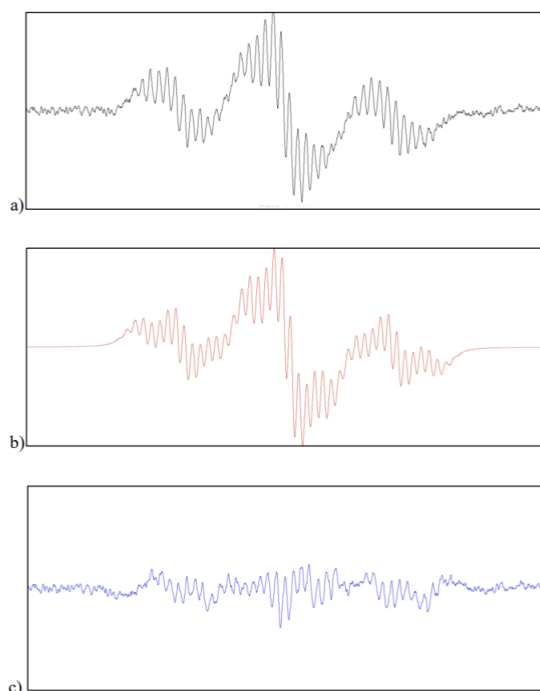


Figure 6: Fast Flow ESR spectrum of 4-tert-butylphenol derived radicals. The concentrations of components in the flat cell were: 4-tert-butylphenol and 0.9mM Ce(SO₄)₂. A) is the experimental spectrum with the parameters: 9.384839 GHz microwave frequency, 3344.31G center field \pm 15G, 0.7G modulation width, 1.0 second time constant, 20mW microwave power, 15min sweep time for a total of 1 sweep, 100ml/min flow rate, and 2000 receiver gain. B) is the simulated spectrum with species having the following coupling

constants: $a^{\text{H}_i} = 6.08$ (2H), $a^{\text{H}_i} = 1.85$ (2H), $a^{\text{H}_{\text{CH}}} = 0.46$ (9H). c) is the residual from the simulated spectrum. The 3 spectra are on the same vertical scale.

4-Vinyl phenol

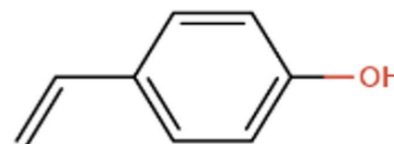


Figure 7: Chemical structure of 4-Vinyl phenol

Fast flow experimentation of 4-Vinyl phenol produced a signal in ESR, indicating the formation of radicals. The fast flow experiment consisted of two solutions. The first solution consisted of 2mM 4-Vinyl phenol in a 50/50 (v/v) ration solution of DI H₂O and 95% ethanol. The second solution consisted of 1.8mM Ce(SO₄)₂ in 0.225M concentrated H₂SO₄. Equivalent volumes were mixed in the flat cell, creating final concentrations of 1.0mM 4-Vinyl phenol and 0.9mM Ce(SO₄)₂. An ESR signal was observed at the flow rate of 55mL/min. This flow rate of 55mL/min produced the best ESR signal, which can be seen in Figure 8(a). Additionally, Figure 8(b) shows the simulated spectrum in WinSim that has a correlation value of $R^2=0.974033$. Four distinct coupling constants were able to be extracted: $a^{\text{H}_i} = 6.80$ (2H), $a^{\text{H}_i} = 1.36$ (2H), $a^{\text{H}_{\text{CH}}} = 2.75$ (1H), and $a^{\text{H}_{\text{CH}_2}} = 5.15$ (2H). Also, a second species was added to the simulation, since

polymerization was possible. The addition of a second species improves the correlation value when optimizing coupling constants. The parameters for species 1 are as follows: 35.747% relative concentration, 73.463G Lorentzian line shape, 0.491G line width, and 0.000G G-shift. The parameters for species 2 are as follows: 64.253% relative concentration, -95.567G Lorentzian line shape, 4.761G line width, and 0.000G G-shift. These parameters were optimized in WinSim software. In Figure 8(c) a residual spectrum is shown, which is generated by 14 subtracting the experimental spectrum from the simulated spectrum. The residual spectrum displays a fair amount of noise, which could be caused by the second species. The noise is relatively symmetrical without many large peaks, which can be predicted by the high correlation value.

DFT calculations were facilitated using the "epr-ii" basis set, which is a variation of the 3-21G basis set. The calculations produced the following coupling constants: $a^{\text{H}_\text{H}} = 6.24$ (2H), $a^{\text{H}_\text{H}} = 2.66$ (2H), $a^{\text{H}_\text{CH}} = 2.93$ (1H), and $a^{\text{H}_\text{CH}_2} = 7.35$ (2H).

These results are summarized in Table 1. These results demonstrate that through the chemical oxidation of 4-Vinyl phenol, stable phenoxyl radicals form that live long enough to be observed using specific parameters in our experimentation. Among all the experimental couplings, only the two ortho-position hydrogens exhibited values higher than those predicted by DFT calculations. While the experimental coupling constants deviate slightly from the predicted DFT couplings, the two groups of values are similar enough to validate our results.

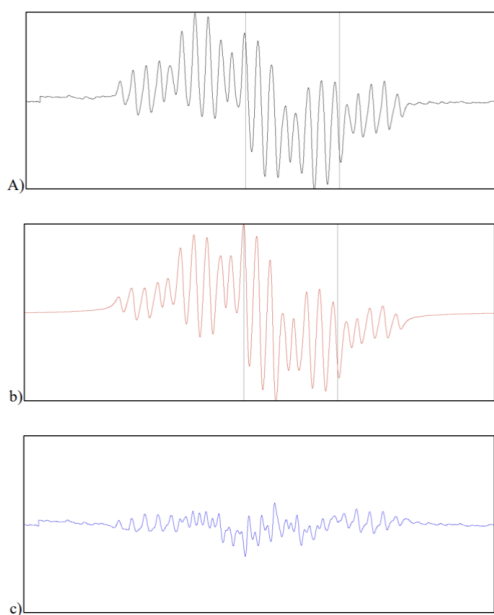


Figure 8: Fast Flow ESR spectrum of 4-vinyl phenol derived radicals. The concentrations of components in the flat cell were: 1.0mM 4-vinyl phenol and 0.9mM Ce(SO₄)₂. A) is the experimental spectrum with the parameters: 9.390472 GHz microwave frequency, 3348.55G center field \pm 25G, 0.5G modulation width, 0.3 second time constant, 22mW microwave power, 2min sweep time for a total of 16 sweeps, 55ml/min flow rate, and 4000 receiver gain. B) is the simulated spectrum with $R^2=0.974033$. The simulation contained

two species, with the first species having the following coupling constants: $a^{\text{H}_\text{H}} = 6.80$ (2H), $a^{\text{H}_\text{H}} = 1.36$ (2H), $a^{\text{H}_\text{CH}} = 2.75$ (1H), and $a^{\text{H}_\text{CH}_2} = 5.15$ (2H). c) is the residual from the simulated spectrum. The 3 spectra are on the same vertical scale.

4-Hydroxybenzalacetone

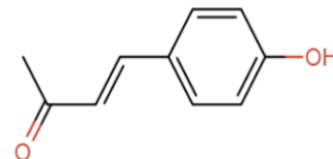


Figure 9: Chemical structure of 4-Hydroxybenzalacetone

Fast flow experimentation of 4-hydroxybenzalacetone produced a signal in ESR, indicating the formation of radicals. The fast flow experiment consisted of two solutions. The first solution consisted of 5mM 4-hydroxybenzalacetone in a 50/50 (v/v) ratio solution of DI H₂O and 95% ethanol. The second solution consisted of 4.8mM Ce(SO₄)₂ in 0.225M concentrated H₂SO₄. Equivalent volumes were mixed in the flat cell, creating final concentrations of 2.5mM 4-hydroxybenzalacetone and 2.4mM Ce(SO₄)₂. An ESR signal was observed at flow rates of 20mL/min, 55mL/min, 85mL/min, and 100mL/min. A flow rate of 100mL/min produced the best ESR signal, which can be seen in Figure 10(a). Additionally, Figure 10(b) shows the simulated spectrum in WinSim that has a correlation value of $R^2=0.969228$. Five distinct coupling constants were able to be extracted: $a^{\text{H}_\text{H}} = 5.35$ (2H), $a^{\text{H}_\text{H}} = 1.71$ (2H), $a^{\text{H}_\text{CH}} = 3.09$ (1H), $a^{\text{H}_\text{CH}} = 7.12$ (1H), and $a^{\text{H}_\text{CH}_3} = 0.051$ (3H). A second species was added to the simulation, since polymerization was possible. The addition of a second species improves the correlation value when optimizing coupling constants. The parameters for species 1 are as follows: 63.589% relative concentration, -69.049G Lorentzian line shape, 0.410G line width, and 0.000G G-shift. The parameters for species 2 are as follows: 36.411% relative concentration, 214.360G Lorentzian line shape, 4.479G line width, and 0.000G G-shift. These 17 parameters were optimized in WinSim software. In Figure 10(c), a residual spectrum is shown, which is generated by subtracting the experimental spectrum from the simulated spectrum. The residual spectrum

exhibits a consistent yet pronounced level of noise. Its level distribution along the x-axis suggests a reasonably good fit between the simulated and experimental spectra. However, the prominent residual noise indicates that the correlation is not perfect and could be further optimized.

DFT calculations were facilitated using the “epr-ii” basis set, which is a variation of the 3-21G basis set. The calculations produced the following coupling constants: $a^{\text{H}_\text{H}} = 6.11$ (2H), $a^{\text{H}_\text{H}} = 2.78$ (2H), $a^{\text{H}_\text{CH}} = 3.40$ (1H), $a^{\text{H}_\text{CH}} = 7.12$ (1H), and $a^{\text{H}_\text{CH}_3} = 0.1$ (3H). These results are summarized in Table 1.

These results demonstrate that through the chemical oxidation of 4-hydroxybenzalacetone, stable phenoxyl radicals form that live long enough to be observed using specific parameters in our experimentation. The experimental coupling constants are smaller than the couplings obtained through DFT calculations. The two groups of couplings constants are < 1.0G of a difference from each other, indicating that the experimental couplings are valid. Moreover, similar trends in coupling constants for specific positions can be seen from the first three molecules studied. The two ortho-position hydrogens exhibit a coupling constant of approximately 6.0 Gauss, while the meta-position hydrogens yield a significantly lower value of around 1.60 Gauss. Additionally, both 4-vinyl phenol and 4-hydroxybenzalacetone show a large coupling between 5.15 and 6.36 Gauss at the vinyl position. DFT calculations predicted these position-specific similarities among these molecules.

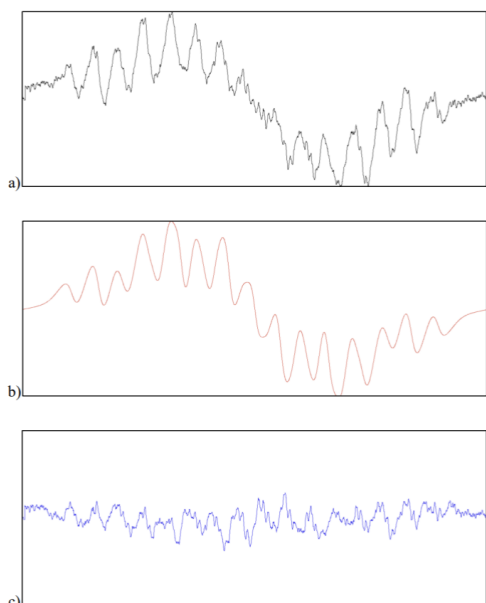


Figure 10: Fast Flow ESR spectrum of 4-hydroxybenzalacetone derived radicals. The concentrations of components in the flat cell were: 2.5mM 4-hydroxybenzalacetone and 2.4mM $\text{Ce}(\text{SO}_4)_2$. A) is the experimental spectrum with the parameters: 9.390486 GHz microwave frequency, 3346.70G center field \pm 15G, 0.7G modulation width, 0.1 second time constant, 5mW microwave power, 2min sweep time for a total of 1 sweep, 100ml/min

flow rate, and 2000 receiver gain. B) is the simulated spectrum with $R^2=0.969228$. The simulation contained two species, with the first species having the following coupling constants: $a^{\text{H}_\text{H}} = 5.35$ (2H), $a^{\text{H}_\text{H}} = 1.71$ (2H), $a^{\text{H}_\text{CH}} = 3.09$ (1H), $a^{\text{H}_\text{CH}} = 6.36$ (1H), $a^{\text{H}_\text{CH}_3} = 0.051$ (3H). c) is the residual from the simulated spectrum. The 3 spectra are on the same vertical scale.

Ferulic acid

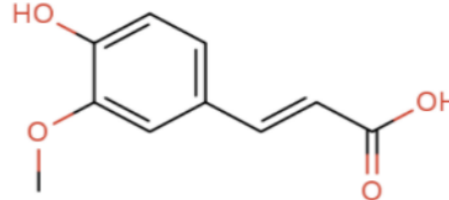


Figure 11: Chemical structure of ferulic acid.

Fast flow experimentation of ferulic acid produced a signal in ESR, indicating the formation of radicals. The fast flow experiment consisted of two solutions. The first solution consisted of 5mM ferulic acid in a 50/50 (v/v) ration solution of DI H₂O and 95% ethanol. The second solution consisted of 4.8mM $\text{Ce}(\text{SO}_4)_2$ in 0.225M concentrated H₂SO₄. Equivalent volumes were mixed in the flat cell, creating final concentrations of 2.5mM ferulic acid and 2.4mM $\text{Ce}(\text{SO}_4)_2$. An ESR signal was observed at a flow rate of 60mL/min., which produced an ESR signal seen in Figure 12(a). Additionally, Figure 12(b) shows the simulated spectrum in WinSim that has a correlation value of $R^2 = 0.936528$. Six distinct coupling constants were able to be extracted: $a^{\text{H}_\text{H}} = 1.95$ (3H), $a^{\text{H}_\text{H}} = 5.25$ (1H), $a^{\text{H}_\text{H}} = 2.66$ (1H), $a^{\text{H}_\text{H}} = 0.56$ (1H), $a^{\text{H}_\text{CH}} = 1.48$ (1H), and $a^{\text{H}_\text{CH}} = 4.15$ (1H). A second species was introduced to the simulation since ferulic acid has trans and cis isomeric forms, which could affect coupling constants. The parameters for species 1, the trans isomer, are as follows: 55.975% relative concentration, 100.701G Lorentzian line shape, 0.213G line width, and 0.000G G-shift. The parameters for species 2 are as follows: 44.025% relative concentration, 105.006G Lorentzian line shape, 0.316G line width, and 0.000G G-shift. These parameters were optimized in WinSim software. In Figure 12(c) a residual spectrum is shown, which is generated by subtracting the experimental spectrum from the 20 simulated spectrum. The residual spectrum displays a substantial amount of remaining signal, particularly concentrated as sharp peaks in the central region. This elevated signal aligns with the moderate correlation coefficient ($R^2 = 0.936528$), indicating that the fit is reasonable, but can be improved for greater accuracy.

DFT calculations were facilitated using the “epr-ii” basis set, which is a variation of the 3-21G basis set. The calculations produced the following coupling constants: $a^{\text{H}_\text{H}} = 3.39$ (3H), $a^{\text{H}_\text{H}} = 4.69$ (1H), $a^{\text{H}_\text{CH}} = 2.50$ (1H), $a^{\text{H}_\text{H}} = 1.37$ (1H), $a^{\text{H}_\text{CH}} = 2.47$ (1H),

and $a^{\text{H}_{\text{CH}}} = 5.22$ (1H). These results are summarized in Table 1.

These results demonstrate that through the chemical oxidation of ferulic acid, stable phenoxyl radicals form that live long enough to be observed using specific parameters in our experimentation. The alignment between the experimental and DFT-derived coupling constants is a little more widespread, as some positions are smaller or larger than the predicted values. The fact that trans and cis isomers could be existing in the flat cell would suggest some variability in the optimized experimental coupling constants.

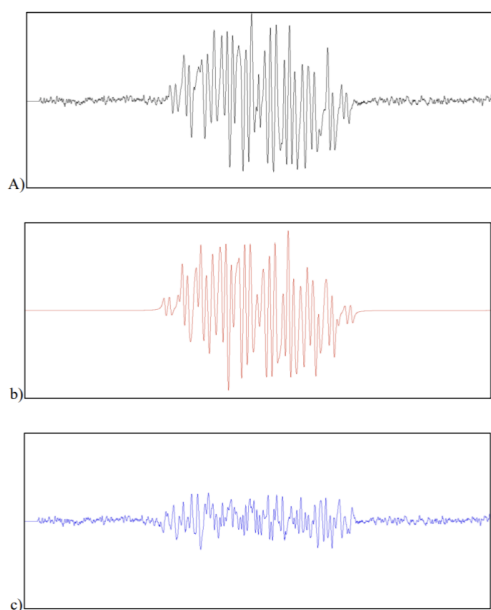


Figure 12: Fast Flow ESR spectrum of ferulic acid derived radicals. The concentrations of components in the flat cell were: 2.5mM ferulic acid and 2.4mM $\text{Ce}(\text{SO}_4)_2$. A) is the experimental spectrum with the parameters: 9.390255 GHz microwave frequency, 3344.77G center field $\pm 25\text{G}$, 0.25G modulation width, 0.3 second time constant, 16mW microwave power, 8min sweep time for a total of 6 sweeps, 60ml/min flow rate, and 2000 receiver gain. B) is the simulated spectrum with $R^2=0.936528$. The simulation contained

two species, with the first species having the following coupling constants: $a^{\text{H}_i} = 1.95$ (3H),

$a^{\text{H}_{\text{H}}} = 5.25$ (1H), $a^{\text{H}_{\text{CH}}} = 2.66$ (1H), $a^{\text{H}_{\text{H}}} = 0.56$ (1H), $a^{\text{H}_{\text{CH}}} = 1.48$ (1H), and $a^{\text{H}_{\text{CH}}} = 4.15$ (1H).

C) is the residual from the simulated spectrum. The 3 spectra are on the same vertical scale.

Bisdemethoxycurcumin

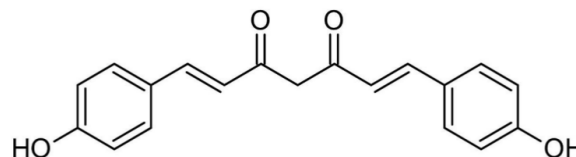


Figure 13: Chemical structure of Bisdemethoxycurcumin

Fast flow experimentation of bisdemethoxycurcumin produced a signal in ESR, indicating the formation of radicals. The fast flow experiment consisted of two solutions. The first solution consisted of 2mM bisdemethoxycurcumin in a 50/50 (v/v) ratio solution of DI H₂O and 95% ethanol. The second solution consisted of 1.8mM $\text{Ce}(\text{SO}_4)_2$ in 0.225M concentrated H₂SO₄. Equivalent volumes were mixed in the flat cell, creating final concentrations of 1mM bisdemethoxycurcumin and 0.9mM $\text{Ce}(\text{SO}_4)_2$. An ESR signal was observed at flow rates of 55mL/min and 70mL/min. A flow rate of 70mL/min produced the best ESR signal as seen in Figure 14(a). Additionally, Figure 14(b) shows the simulated spectrum in WinSim that has a correlation value of $R^2=0.972305$. Five distinct coupling constants were able to be extracted: $a^{\text{H}_{\text{H}}} = 1.44$ (4H), $a^{\text{H}_{\text{H}}} = 1.48$ (4H), $a^{\text{H}_{\text{CH}}} = 3.06$ (2H), $a^{\text{H}_{\text{CH}}} = 5.11$ (2H), and $a^{\text{H}_{\text{CH}_2}} = 2.75$ (2H). A second species was added to the simulation since polymerization could occur due to the low solubility of bisdemethoxycurcumin. The parameters for species 1 are as follows: 8.698% relative concentration, 9.780G Lorentzian line shape, 0.240G line width, and 0.000G G-shift. The parameters for species 2 are as follows: 91.302% relative concentration, 21.715G Lorentzian line shape, 6.241G line width, and 0.000G G-shift. These parameters were optimized in WinSim software. In Figure 14(c) a residual spectrum is shown, which is generated by 23 subtracting the experimental spectrum from the simulated spectrum. The residual spectrum displays a relatively low amount of noise, indicating a good fit for the simulated and experimental spectra. DFT calculations were facilitated using the “epr-ii” basis set, which is a variation of the 3-21G basis set. The calculations produced the following coupling constants: $a^{\text{H}_{\text{H}}} = 0.82$ (4H), $a^{\text{H}_{\text{H}}} = 1.75$ (4H), $a^{\text{H}_{\text{CH}}} = 2.76$ (2H), $a^{\text{H}_{\text{CH}}} = 4.29$ (2H), and $a^{\text{H}_{\text{CH}_2}} = 12.04$ (2H).

These results are summarized in Table 1. These results demonstrate that through the chemical oxidation of bisdemethoxycurcumin, stable phenoxyl radicals form that live long enough to be observed using specific parameters in our experimentation.

While it remains uncertain whether both phenol rings engage in hyperfine interactions with the unpaired electron, including both rings in the simulation yields the highest correlation value. However, the DFT-predicted coupling constant for the methylene hydrogens ($a^{\text{H}_{\text{CH}_2}} = 12.04$ for 2H) appears unusually large. These hydrogens are distant from the oxidized region and are unlikely to exhibit such strong coupling. A coupling of 12.04 Gauss would simply not fit in the simulated spectrum; it is too large. Furthermore, this value deviates significantly from coupling constants observed in the related molecules, suggesting the possibility that a calculation error occurred. In contrast, the remaining predicted coupling constants align with experimental data, all falling between a ± 1.0 Gauss margin. This provides credibility to the experimental coupling constants

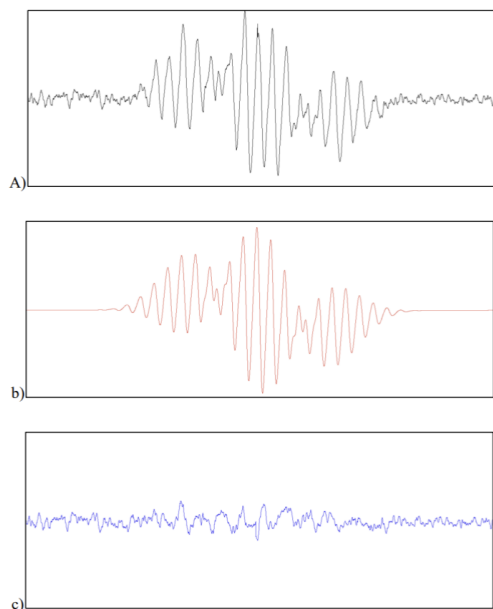


Figure 14: Fast Flow ESR spectrum of bisdemethoxycurcumin derived radicals. The concentrations of components in the flat cell were: 1mM bisdemethoxycurcumin and 0.9mM $\text{Ce}(\text{SO}_4)_2$. A) is the experimental spectrum with the parameters: 9.389304 GHz microwave frequency, 3347.27G center field $\pm 25\text{G}$, 0.5G modulation width, 0.3 second time constant, 16mW microwave power, 4min sweep time for a total of 7 sweeps, 70ml/min flow rate, and 5000 receiver gain. B) is the simulated spectrum with $R=0.972305$. The simulation contained two species, with the first species having the following coupling constants: $a^{\text{H}_{\text{H}}} = 1.44$ (4H), $a^{\text{H}_{\text{H}}} = 1.48$ (4H), $a^{\text{H}_{\text{CH}}} = 3.06$ (2H), $a^{\text{H}_{\text{CH}}} = 5.11$ (2H), and $a^{\text{H}_{\text{CH}_2}} = 2.75$ (2H). C) is the residual from the simulated spectrum. The 3 spectra are on the same vertical scale.

Curcumin

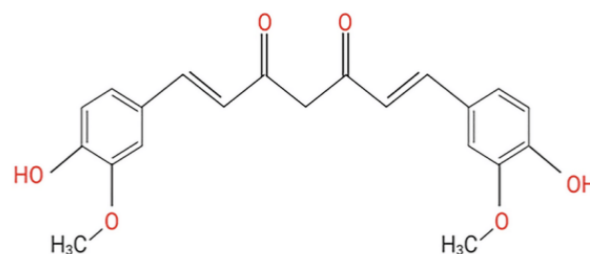


Figure 15: Chemical structure of curcumin.

Fast flow experimentation of curcumin produced a signal that was observable in the ESR instrument. Different concentrations of curcumin were used for the several ESR experiments that were conducted. In trial 1, a 2mM curcumin concentration was used. A concentration of 2mM was used in early trials due to curcumin's relatively low solubility. Thus, in trial 1, the first solution consisted of 2mM curcumin in a 50/50 (v/v) ratio solution of DI H₂O and 95% ethanol. The second solution consisted of 1.8mM $\text{Ce}(\text{SO}_4)_2$ in 0.225M concentrated H₂SO₄. Equal volumes were mixed so the final concentrations of components in the flat cell were 1.0mM resveratrol and 0.9mM $\text{Ce}(\text{SO}_4)_2$. An observable ESR spectrum was observed at flow rates of 50ml/min, 70ml/min, and 100ml/min. Figure 16(a) shows the first ESR spectrum of curcumin with a 2mM concentration. In a later trial, the concentration of curcumin was increased to 5mM to test whether the signal would increase, leading to greater resolution in curcumin spectra. As a result, in trial 3, the first solution consisted of 5mM curcumin in 4L of 95% ethanol. The second solution consisted of 4.8mM $\text{Ce}(\text{SO}_4)_2$ in 0.225M concentrated H₂SO₄. Equal volumes were mixed so the final concentrations of components in the flat cell were 2.5mM curcumin and 2.4mM $\text{Ce}(\text{SO}_4)_2$. An observable ESR spectrum was observed at flow rate of 50mL/min. Figure 16(b) shows the experimental curcumin spectrum from trial 3.26 DFT calculations were unable to be performed for curcumin, as a software issue occurred. This specific software issue occurs with a buildup of previous DFT submissions "scratch files" ending abnormally, leading to all future submissions to fail. To fix this, one can delete all the previous "scratch files", restart Gaussian '03 and GaussView '03, and build the molecule of interest in a new file in GaussView '03; however, when initially trying this fix, files were still unable to be submitted. Moreover, the project timeline did not permit any more time to investigate the problem. Thus, DFT calculations were unable to be obtained. The experimental spectra in Figure 16 demonstrates that through chemical oxidation, curcumin derived phenoxyl radicals' form. While the resolution of the spectra is poor, the large splitting in

the center region shows that there are more potential splittings in that region. To resolve these potential splittings, a stronger signal is needed, and the right parameters are also needed. To achieve this, a little trial and error are required. Therefore, more work can be done to resolve these curcumin spectra so that they can be simulated for coupling constants.

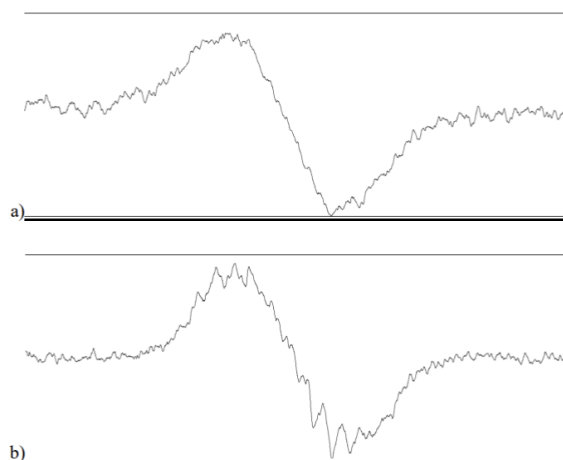


Figure 16: Fast Flow ESR spectrum of curcumin derived radicals. In spectrum (a), The concentrations of components in the flat cell were: 1mM curcumin and 0.9mM Ce(SO₄)₂. A) is the experimental spectrum of trial 1 with the parameters: 9.389701 GHz microwave frequency, 3347.97G center field \pm 25G, 0.5G modulation width, 0.3 second time constant, 16mW microwave power, 2min sweep time for 1 sweep, 100ml/min flow rate, and 3000 receiver gain. B) is the experimental spectrum of trial 3 with the parameters: 9.389731 GHz microwave frequency, 3347.95G center field \pm 25G, 0.5G modulation width, 1.0 second time constant, 16mW microwave power, 8min sweep time for a total of 4 sweeps, 50ml/min flow rate, and 8000 receiver gain.

Table 1

Compound	Position	Group	Experimental	DFT	Sim. Corr.		
4-tert-Butylphenol 	2,6	a^H_{H}	6.08 (2H)	6.96	0.956231		
	3,5	a^H_{H}	1.85 (2H)	2.59			
	4	a^H_{CH}	0.46 (9H)	0.81			
4-Vinylphenol 	2,6	a^H_{H}	6.80 (2H)	6.24	0.974033		
	3,5	a^H_{H}	1.36 (2H)	2.66			
	7	a^H_{CH}	2.75 (1H)	2.93			
	8	$a^H_{CH_2}$	5.15 (2H)	7.35			
4-Hydroxybenzalacetone 	2,6	a^H_{H}	5.35 (2H)	6.11	0.969228		
	3,5	a^H_{H}	1.71 (2H)	2.78			
	7	a^H_{CH}	3.09 (1H)	3.4			
	8	a^H_{CH}	6.36 (1H)	7.12			
	9	a^H_{CH}	0.051 (3H)	0.1			
Ferulic Acid 	2	a^H_{H}	1.95 (3H)	3.39	0.936528		
	6	a^H_{H}	5.25 (1H)	4.69			
	3	a^H_{H}	2.66 (1H)	2.5			
	5	a^H_{H}	0.56 (1H)	1.37			
	7	a^H_{CH}	1.48 (1H)	2.47			
	8	a^H_{CH}	4.15 (1H)	5.22			
	Bisdemethoxycurcumin 	2,6	a^H_{H}	1.44 (4H)		0.47	0.972305
		3,5	a^H_{H}	1.48 (4H)		1.75	
7		a^H_{CH}	3.06 (2H)	2.76			
8		a^H_{CH}	5.11 (2H)	4.29			
9		$a^H_{CH_2}$	2.75 (2H)	12.04			
Curcumin 		2	a^H_{H}	-	-	-	
	6	a^H_{H}	-	-			
	3,5	a^H_{H}	-	-			
	7	a^H_{CH}	-	-			
	8	a^H_{CH}	-	-			
	9	$a^H_{CH_2}$	-	-			

Conclusion

This study was conducted to observe phenoxyl free radicals of curcumin and other related compounds using electron spin resonance spectroscopy. The compounds studied were 4-tert-Butylphenol, 4-Vinyl phenol, 4-Hydroxybenzalacetone, Ferulic acid, Bisdemethoxycurcumin, and Curcumin. Each of the molecules produced observable free radicals when oxidized. While all the molecules produced free radicals, curcumin radicals were unable to be simulated with a high correlation. This was likely a result of polymerization that created a second species, affecting the ESR spectra. For the molecules able to be simulated, they were done so in WinSim, yielding coupling constants. DFT calculations were successfully performed for all molecules except curcumin, which was excluded due to software-related issues. While the simulated coupling constants did not exactly match the DFT predicted coupling constants, there appeared to be trends in coupling constant values for certain positions among most of the molecules. As research continues in the dietary supplement industry for products efficacy and safety, the proposed benefits and properties of these products will remain a topic of ongoing discussion. For this topic,

more ESR research can be done with curcumin to try and resolve spectra so that they can be simulated for coupling constants. Modifications such as altering the oxidizing agent or adjusting the experimental apparatus to minimize polymerization may be explored to improve curcumin spectra resolution.

REFERENCES

- (1) Sipe Jr., Herbert J., Free Radicals, Liver Toxicology, ESR Lecture Notes and Handouts. 2025. <https://doi.org/10.1007/s11746-998-0032-9>.
- (2) Aruoma, Okezie I. "Free Radicals, Oxidative Stress, and Antioxidants in Human Health and Disease." *Journal of the American Oil Chemists' Society*, vol. 75, no. 2, Feb. 1998, pp. 199–212, <https://doi.org/10.1007/s11746-998-0032-9>.
- (3) Rajashekar, Channa B. "Dual Role of Plant Phenolic Compounds as Antioxidants and Prooxidants." *American Journal of Plant Sciences*, vol. 14, no. 01, 2023, pp. 15–28, <https://doi.org/10.4236/ajps.2023.141002>.
- (4) Peng, Ying, et al. "Anti-Inflammatory Effects of Curcumin in the Inflammatory Diseases: Status, Limitations and Countermeasures." *Drug Design, Development and Therapy*, vol. 15, Nov. 2021, pp. 4503–4508, <https://doi.org/10.2147/DDDT.S327378>.
- (5) Gerson, F., & Huber, W. *Electron Spin Resonance Spectroscopy of Organic Radicals*. Weinheim: Wiley-VCH, 2003. Print.
- (6) Weil, J. A., & Bolton, J. R. *Electron Paramagnetic Resonance: Elementary Theory and Practical Applications*. John Wiley & Sons. 2007.
- (7) Wahl, A. C. Molecular Orbital Densities: Pictorial Studies. *Science* 1966, 151 (3713), 961–967. <https://doi.org/10.1126/science.151.3713.961>.
- (8) van Mourik, T.; Bühl, M.; Gageot, M.-P. Density Functional Theory across Chemistry, Physics and Biology. *Philosophical transactions. Series A, Mathematical, physical, and engineering sciences* 2014, 372 (2011). <https://doi.org/10.1098/rsta.2012.0488>.
- (9) Duling, D. R.; Motten, A. G.; Mason, R. P. Generation and Evaluation of Isotropic ESR Spectrum Simulations. *Journal of Magnetic Resonance* (1969) 2004, 77 (3), 504–511. [https://doi.org/10.1016/0022-2364\(88\)90008-X](https://doi.org/10.1016/0022-2364(88)90008-X).
- (10) WinSIM HTML Manual. National Institute of Environmental Health Sciences. <https://www.niehs.nih.gov/research/resources/software/tox-pharm/tools/winsim>
- (11) G03 Manual: G03MANTOP. Gac.edu. http://bohr.chem.gac.edu/docs/g03man/g_ur/g03mantop.htm